Available online at https://www.sjomr.org.in

SCIENTIFIC JOURNAL
OF MEDICAL RESEARCH

Vol. 7, Issue 25, pp 1-8 , 2023

ISSN: 2520-5234

RESEARCH ARTICLE

Assessment of the anti-bacterial and antioxidant activity of silver nanoparticles produced by oil field reservoirs bacterium

Hasan G. A. Alshami[1], Rashid R. Hateet[2], Wijdan H. Al-Tamimi[1]

[1]Department of Biology, College of Science, University of Basrah, Basrah, Iraq.
[2]Department of Biology, College of Science, University of Misan, Maysan, Iraq.

ARTICLE INFORMATIONS

Article history:
Received: 28 December 2022
Revised: 22 January 2023
Accepted: 7 February 2023
Published: 24 March 2023

Keywords:
Anti-bacterial, Antioxidant, *Bacillus cereus*, Biosynthesis, Silver nanoparticles, MDR

Corresponding author:
Hasan G. A. Alshami
Email: pgs2100@uobasrah.edu.iq
Department of Biology, College of Science, University of Basrah, Basrah, Iraq

ABSTRACT

Objective: This study aimed to synthesize, characterize, and evaluate the anti-bacterial and antioxidant activity of silver nanoparticles (AgNPs) synthesized using the supernatant of *Bacillus cereus* strain DBA1.1 isolated from an oil field reservoir.

Methods: The Uv-visible (Uv-vis) spectrophotometer, X-ray diffraction (XRD), transmission electron microscopy (TEM), scanning electron microscopy (SEM), atomic force microscopy (AFM), and zeta potential analysis were used to characterize the synthesized AgNPs. By utilizing the agar well diffusion technique, the anti-bacterial efficacy of AgNPs was assessed against multidrug-resistant (MDR) bacteria isolated from human urinary tract infections (UTI). The antioxidant activity of AgNPs was investigated using the 1,1-diphenyl-2-pyridylhydrazine (DPPH) test.

Results: The results indicate the formation of AgNPs through the visual observations of dark brown color, which UV absorption at 432 nm further confirms this. The fabricated AgNPs had a spherical shape, and the average size was found to be 20.83, 17.47, and 18.11 nm according to XRD analyses, TEM, and SEM, respectively. In AFM, AgNPs were measured to have a mean diameter of about 65 nm. The mean negative zeta potential of AgNPs was -14.5 mV. AgNPs demonstrated significant anti-bacterial properties against MDR bacteria depending on concentration, with the highest diameter inhibition zone of 24.33 ± 0.57 mm against *Staphylococcus haemolyticus* at a concentration of 1000µg/mL. Powerful antioxidant activity was noticed, with an IC_{50} value of 112.16 µg/mL.

Conclusions: The present work concluded that synthesized AgNPs were spherical, monodisperse, stable, and within acceptable sizes. They may be good candidates for further biological applications.

INTRODUCTION

Nanotechnology creates a variety of nanoscale materials with a size of 1–100 nanometers in at least one dimension; these materials are known as nanomaterials or nanoparticles (NPs).[1] It is a modern technique that includes the production, characterization, and application of NPs,2 which has the potential to revolutionize the medical sector by providing novel tools for infection treatment and early diagnosis of

CITATION: Alshami HGA, Hateet RR, Al-Tamimi WH. Assessment of the anti-bacterial and antioxidant activity of silver nanoparticles produced by oil field reservoirs bacterium. Sci. J. Med. Res. 2023;7(25):1-8. DOI: 10.37623/sjomr.v07i25.01

contagious illnesses.3 Due to the fabrication and various applications of NPs in multiple fields such as biology, agriculture, engineering, electronics, cosmetics, medicine, and biomedical devices, nanotechnology has evolved significantly in recent decades. NPs have gotten attention due to their unique physicochemical properties and important biotechnological applications.[4,5] NPs are synthesized in one of two ways: "top-down" or "bottom-up." In the first method, large materials are subdivided into smaller molecules through various physical and chemical methods. In contrast, in the latter method, NPs are formed by self-assembling atoms in the nucleus and then transformed into NPs. This method involves chemical and biological approaches.6,7 The physical and chemical methods are expensive and environmentally unfriendly, restricting the use of NPs in biological and medical applications. Therefore easy, low-cost, and eco-friendly methods are required to overcome the limits of physiochemical techniques for the production of these NPs without the use of harmful and expensive chemicals and solvents.[8] As a result, biological synthesis has gotten a lot of attention.[9] Biological synthesis means using plants and microorganisms to synthesize NPs.[10] Because of growing success, ease of handling, and alteration in the genetic material, bacterial utilization is gradually gaining significance among microorganisms.[11] Bacterial utilization in nanotechnology research began in the late 1990s, and it has expanded since then.[12] Numerous bacteria were employed to produce multiple NPs, including the biosynthesis of AgNPs via *Bacillus licheniformis* TT01 [13], *Actinobacteria Rhodococcus* NCIM 2891, 14 copper nanoparticles (CuNP) by *Pseudomonas silesiensis* [15], and gold nanoparticle (AuNPs) using four bacteria including; *Bacillus subtilis*, *Lactobacillus acidophilus, Escherichia coli*, and *Streptococcus thermophiles*.[16]

Humanity is currently faced with two issues: (i) multidrug-resistant (MDR) bacteria and (ii) disorders caused by free radicals. Antibiotic resistance is a serious risk to public health that kills about 0.7 million individuals per year, and by 2050, this statistic is likely to climb to 10 million [17]. MDR bacteria cause a large percentage of infections in hospitalized patients.[18] Numerous studies have confirmed AgNPs as a possible solution to the problem of bacterial resistance, owing to their efficacy against a variety of bacteria.[19] Free radicals also play an important role in the occurrence of degenerative disorders in the body, including heart and blood vessel disease, mutations, senescence, and tumorigenesis.[20] AgNPs also can be used to scavenge free radicals instead of antibiotics.[21] This research aimed (i) to manufacture AgNPs using *Bacillus cereus* strain DBA1.1, (ii) to characterize the synthesized AgNPs, and (iii) to evaluate the anti-bacterial and antioxidant efficacy of the synthesized AgNPs.

MATERIALS AND METHODS

The bacterial strain used for the synthesis of AgNPs

In a previous study, nine different bacterial strains were isolated from produced water samples of an oil field reservoir, identified using universal primers (16S rDNA gene), and then screened for AgNP synthesis. Upon screening, it was found that *B. cereus* strain DBA1.1 was the most powerful among the nine strains tested for extracellular AgNP synthesis.[22] so it was used in this study.

Biosynthesis of AgNPs

With some modifications, this method was carried out according to Singh *et al*. The *B. cereus* strain DBA1.1 has been inoculated in a flask with 100 ml of sterile nutrient broth (NB). The culture was centrifuged at 6000 rpm for 10 minutes using a Table Top Centrifuge (Gemmy, Taiwan) after 24 hours of incubation at 37°C in an orbital shaker (150 rpm) to get the supernatant. In a 250 mL conical flask, 100 mL of silver nitrate ($AgNO_3$) solution (1 mM) was added to the culture supernatant. The flask was then covered with aluminum foil and incubated at 37°C for three days at 150 rpm. A medium agNO3 solution mixture was used as a control. The supernatant was visually noticed for any development in color during the formation of AgNPs.[23]

Characterization of the synthesized AgNPs

UV–Vis spectrophotometer

To prove the fabrication of AgNPs, the culture supernatant was examined by a Dual Beam UV-1800 Spectrometer (Shimadzu, Japan) with a wavelength range of 200–800 nm. Using deionized water, AgNPs were cleaned 3 times by centrifugation at 10000 rpm for 10 minutes each time, then air-dried and collected as a powder[19]

The X-ray diffraction (XRD) analyses

The X'pert Pro X-ray diffract meter (PANalytical, Netherlands) was employed to measure the XRD of AgNPs produced by *B. cereus* strain DBA1.1. The diffraction pattern of the powdered form of synthesized NPs was recorded from 10° to 80° (2 theta), with a step size of 0.050°, by Cu K-Alpha radiation (k = 1.54060 Å) and operating at 40 kV and 30 mA. Scherer's equation was applied to find the average crystalline size of the NPs as previously described.[24]

Transmission electron microscopy (TEM)

TEM was used to analyze the shape, size, and distribution of NPs. In order to prepare the TEM grid, the suspension of AgNPs was transferred onto a copper grid coated with carbon. Before imaging, the grid was dried by air, and then individual images were taken at 200 kV using TEM [24].

Scanning electron microscopy (SEM)

The morphology traits of the synthesized AgNPs were observed by SEM (MIRA3 LMU TESCAN, Czech). A small drop of AgNPs suspension was added to the slide and allowed to dry before being analyzed by SEM. The microscope operated at different magnification.[25]

Atomic force microscopy (AFM)

The size and morphology of AgNPs were characterized by

the AFM device (Nanosurf easyScan 2 AFM, Switzerland). Before the AFM scanning, a thin film of bio-fabricated AgNPs was coated on a clean glass coverslip and permitted to dry at room temperature.[26]

Zeta potential analysis

The zeta potential method was utilized to assess the stability of *B. cereus* strain DBA1.1 mediated synthesized AgNPs using a zeta potential analyzer instrument (HORIBA Scientific SZ-100, Japan). For this analysis, the sample was centrifuged, and the NPs were measured between -200 and +200 mV at 25.2ºC.[27]

Anti-bacterial activity of the synthesized AgNPs

The anti-bacterial properties of manufactured AgNPs were assessed against multidrug resistance (MDR) bacteria isolated from human urinary tract infections (UTI). Urine specimens collection and isolation of bacteria were done as reported by Al-Naqshbandi *et al.*[28] Antibiotic susceptibility pattern for detection of MDR bacteria was done using the disk diffusion technique according to Mollick *et al.*[29] and the results (the data not shown) were interpreted according to the guideline of the Clinical Laboratory Standards Institute (CLSI) 2021.[30] MDR bacteria are those that are resistant to at least one agent from three or more antimicrobial classes.[31] Activity of AgNPs was tested against MDR bacteria, including Gram-positive (2 *Enterococcus faecalis*,2 *Staphylococcus hominis*, *Staphylococcus aureus*, *Staphylococcus hemolyticus*) and Gram-negative bacteria (6 *Escherichia coli*, 3 *Klebsiella pneumoniae*, *Klebsiella oxytoca*) by agar well diffusion technique. In nutrient broth (NB), pure colonies of bacteria were grown at 37°C for 24 hrs, and the turbidity was adjusted to 0.5 McFarland standard using sterile distilled water. Separate Mueller Hinton agar (MHA) plates were swabbed uniformly with every type of bacteria, and wells were punched in each plate with a 7 mm sterilized cork borer. A total of 100 µL of AgNPs dissolved in dimethyl sulfoxide (DMSO) at concentrations of 100, 250, 500, and 1000 µg/ml were poured into each well, along with the control (DMSO only), and plates were incubated at 37ºC for 24 hours. Following the incubation, the inhibition zone diameters surrounding each well were calculated in millimeters (mm) using a clear plastic ruler.[32]

Antioxidant activity of the synthesized AgNPs

By using the 1,1-diphenyl-2-pyridyl-hydrazine (DPPH) assay, the antioxidant potential of AgNPs was measured in terms of free radical scavenging activity (RSA) as stated by Mujaddidi *et al.*[20] Briefly, in DMSO solution, different concentrations of AgNPs (5, 10, 25, 50, 100, 200, 400 µg/ ml) were prepared. In glass test tubes, 1 ml of each concentrate was mixed with 1 ml of a 0.004 % methanolic DPPH free radical solution. The test tubes were then incubated in the dark for 30 minutes at room temperature, and the absorbance (Abs) at 517 nm was measured using spectrophotometer (EMC LAB, Germany). The negative and positive controls were DPPH solution/methanol mixture and ascorbic acid, respectively. The antioxidant activity of AgNPs was calculated from the following formula:

$$\text{Inhibition \%} = [(\text{Abs of control} - \text{Abs of sample}) / \text{Abs of control}] \times 100 \quad (1)$$

Statistical Analysis

The agar well diffusion technique and DPPH assay were carried out in triplicate, and the data were analyzed using IBM Statistical Package for the Social Sciences (SPSS) software version 26 to determine mean values, standard deviation (means ± SD), and significance between means. Data were analyzed using analysis of variance (ANOVA), and $p \leq 0.05$ was deemed statistically significant. The size distribution of NPs was analyzed using Image J software. The graphs were plotted using the Origin Pro 2018 software and Microsoft Excel 2010.

RESULTS AND DISCUSSION

Biosynthesis of AgNPs

The biosynthesis of AgNPs was first affirmed by noticing the change in color of *B. cereus* strain DBA1.1 supernatant treated with $AgNO_3$ solution. The color of the supernatant transformed from pale yellow to dark brown following incubation time due to surface plasmon resonance (SPR), while no change was seen in the control (Figure 1). This outcome is in agreement with those reported by Elbeshehy *et al*. and Syed *et al.* in the extracellular synthesis of AgNPs using *Bacillus spp.* and *Aneurinibacillus migulanus* 141.[33,34]

Based on the location of the NPs synthesized, there are two kinds of synthesis methods: intracellular[35] and extracellular.[36] The precise mechanism by which bacteria synthesize NPs is unknown. According to studies, NPs are typically formed by trapping metal ions on the surface or within the bacterial cell. Then, with the enzymes' help, the trapped metal ions are reduced to NPs.[37] Extracellular synthesis is more suitable and simpler than intracellular synthesis because the NPs produced can be easily purified.[38] As a result, we concentrated on extracellular synthesis in the current study.

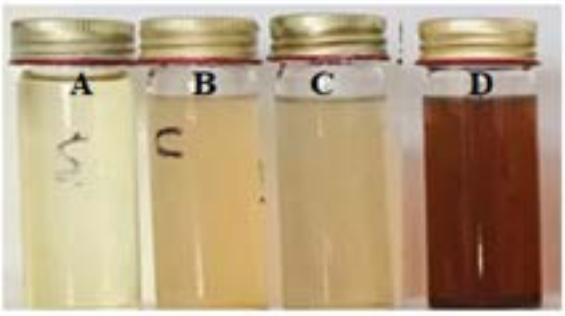

Figure 1: Observation of color change. A: Supernatant only, B: Control (mixture of medium and $AgNO_3$ solution), C: *B. cereus* strain DBA1.1 Supernatant treated with $AgNO_3$ solution before incubation, D: Synthesis of AgNPs after incubation

Characterization of the synthesized AgNPs

After the incubation period, the reduction of $AgNO_3$ to AgNPs by *B.cereus* strain DBA1.1 was made by measuring the UV–Vis spectrum of the supernatant. As depicted in Figure 2, the absorption spectrum of synthesized AgNPs was observed at 432 nm due to the SPR band of the produced AgNPs. This outcome is in complete agreement with previous studies that characterized the AgNPs using the UV-Vis spectrum.[25,39] According to research findings, the peak from 400 to 475 nm corresponds to the SPR of AgNPs.[40,41] As a result, the *B. cereus* strain DBA1.1 supernatant shows the manufacturing of AgNPs.

According to Figure 2, the peak for the supernatant of *B. cereus* strain DBA1 was sharp and high, attributed to the synthesis of homogeneous and monodisperse AgNPs (spherical AgNPs) as previously described by Sathiya and Akilandeswari [39] and Alahmad *et al*.[42] which is proved by the TEM, SEM, and AFM as shown in Figure 4 (a), Figure 5 (a), and Figure 6, respectively.

The crystallinity of the produced AgNPs was evidenced using XRD analyses. Figure 3 shows the XRD patterns of AgNPs produced by *B. cereus* strain DBA1.1 supernatant. The peaks were observed at 2θ = 45.86°, 55.01°, 67.42°, and 76.70°, corresponding to the lattice planes of the crystalline structure of AgNPs (1 0 3), (0 0 6), (1 1 2), and (2 0 1), respectively; these outcomes are in good agreement with the Joint Committee on Powder Diffraction Standards (JCPDS) file NO. 00-041-1402. Besides, XRD patterns exhibited three peaks at 2θ = 27.92°, 32.38°, and 57.32° corresponding to (0 2 1), (2 2 1), and (1 4 2), respectively; these peaks may relate to unreduced $AgNO_3$ during the synthesis process which is well-matched with the JCPDS file NO. 01-070-0779, as stated by Hanna *et al*. [43], may be caused by supernatant biomolecules that cap the synthesized AgNPs [44]. According to Figure 3, all of the peaks are sharp. The capping agents may have stabilized the NPs, resulting in sharp Bragg peaks. Potent Bragg reflections indicate the presence of strong X-ray scattering centers in the crystalline phase, which could be caused by capping agents [38].

Scherrer's equation was used to obtain the average crystalline size of the NPs using the peak position and full width at half-maximum intensity (FWHM) values from the XRD data:

$$D = \frac{k\lambda}{\beta \cos\theta} \qquad (2)$$

where in this equation, D is the crystallite size of the NPs, k is the Scherrer constant, λ is the wavelength of the X-ray source (1.54056 Å) used in XRD patterns, β is the FWHM of the diffraction peaks in radian, and θ is the Bragg angle in radian. Using the above equation, the average crystallite size of the AgNPs is calculated to be 20.83 nm. This result is comparable to a prior study in which the average size of AgNPs produced by *Bacillus cereus* was 21.5 nm, as calculated by the Scherrer equation.[20]

TEM analysis has been demonstrated to be one of the most precise methods to find out the morphology (size and shape) of NPs.[45] The TEM image of synthesized AgNPs confirmed that they were non-agglomerated and spherical in shape (with very few irregular NPs), Figure 4(a). Furthermore, Figure 4(b) depicts the histogram of NPs size distribution, which explains that AgNP sizes were between 8.95 and 33.18 nm, with mean particle sizes of 17.47 nm. Results of previous studies from TEM images largely support the spherical shape of AgNPs produced through the green approach by using different *Bacilli*, such as *B. cereus* [46], *B. subtilis* [40], and *B. licheniformis* [13], with particles size ranging from 19 to 38 nm, 3 to 20 nm, and 2 to 22 nm, respectively. However, the physicochemical properties influence the shape and size of synthesized NPs. The concentration of the metal ion, time, pH, and the temperature of the reaction mixture all play an important role in NPs synthesis [47].

SEM images of the produced AgNPs showed spherical shapes and particle sizes ranging from 13.42 nm to 24.49 nm, Figure 5(a). The histogram of particle size distribution in Figure 5 (b) shows that the mean particle size of AgNPs is 18.11 nm, which is very close to the average size obtained from TEM and XRD analyses. Based on SEM analysis, the spherical shape of *Bacillus*-AgNPs from *B. subtilis* and *B. amyloliquefaciens* with particles sizes ranging from 15.9 to 80 nm, *B. brevis* with particle sizes between 22 and 60 nm, and *B. siamensis* with particle sizes ranging from 25 to 50 nm was also observed by

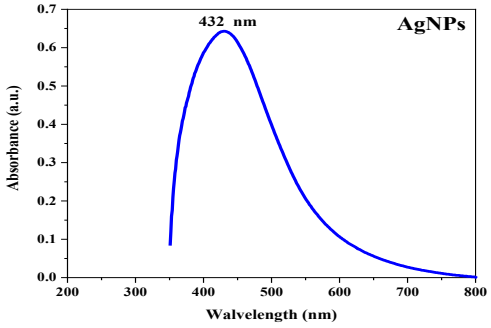

Figure 2: The spectrum of UV-Vis absorption of *B.cereus* strain DBA1.1 AgNPs.

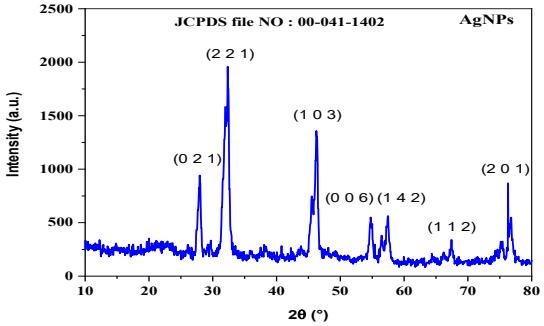

Figure 3: XRD spectra of AgNPs synthesized using *B.cereus* strain DBA1.

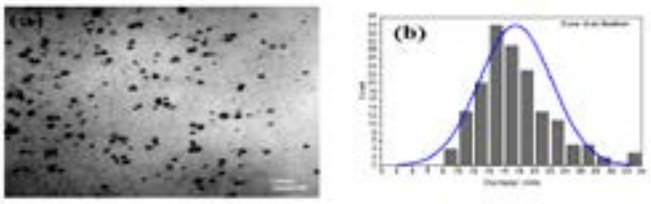

Figure 4: (a) The TEM image of produced AgNPs, and (b) the histogram of particle size distribution from (a) image

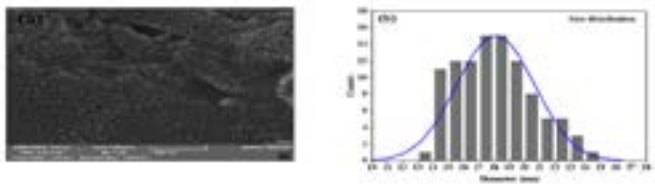

Figure 5: (a) The SEM image of biosynthesized AgNPs and (b) the histogram of particles size distribution from (a) image

Fouad *et al.*[48], Saravanan *et al.*[49], and Ibrahim *et al.*[50].

In AFM, AgNPs were measured to have mean diameters of about 65 nm, with an average roughness of 4.455 nm. Furthermore, the two-dimensional (2D) and three-dimensional (3D) AFM images, as shown in Figure 6, revealed the spherical shape and homogeneous distribution of the synthesized AgNPs achieved by TEM, SEM.

A Zeta potential analysis was conducted to identify the charge on the surface of synthesized AgNPs, which can be used to evaluate the stability of the achieved colloidal AgNPs. The value of the zeta potential shows the possible stability of the particles. The charge on the NPs' surface determines the attractive and repulsive force between them. A negative charge on the surface of NPs is important for long-term stability, as it prevents particle agglomeration in the medium.[27] In the current study, the value of zeta potential proves particle repulsion and thus enhances the stability of produced AgNPs. Figure 7 shows that the NPs' zeta potential mean was -14.5 mV, indicating the stability of the synthesized AgNPs. Elbeshehy *et al.* demonstrated that the Zeta potential of AgNPs produced by *B. licheniformis, B. pumilus*, and *B. persicus* was -21.3, -18.5, and -16.6 mV, respectively [33]. The pH and surface capping agents influence the stability of the NPs.[51]

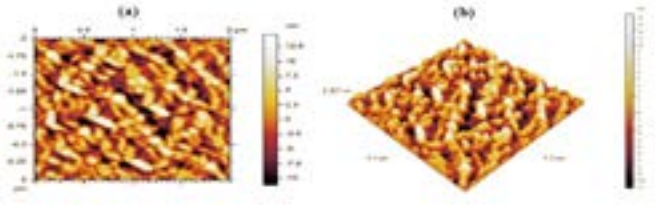

Figure 6: The 2D (a) and 3D (b) AFM images of *B.cereus* strain DBA1.1 AgNPs

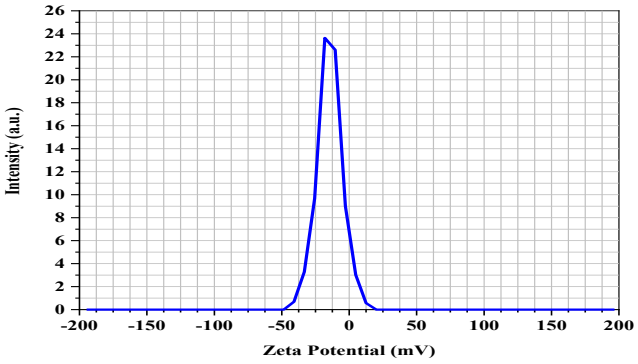

Figure 7: Zeta potential for AgNPs synthesized using the supernatant of *B.cereus* strain DBA1.1

Anti-bacterial activity of the synthesized AgNPs

The anti-bacterial activity results showed that AgNP suspension at various concentrations (100, 250, 500, and 1000 µg/ml) remarkably inhibited the growth of MDR bacteria isolated from UTI when compared to the control (Table 1) and (Figure 8). This activity may be due to the inhibition of translation and protein synthesis, producing high levels of reactive oxygen species (ROS), membrane damage, and release of silver ions (Ag^+) by AgNPs [52,53]. The results of the current study proved that inhibition of bacterial growth increased as the concentration of AgNPs increased. This result is compatible with Ahmed *et al.*, who used different concentrations of AgNPs manufactured from *B.cereus* as anti-bacterial agents [46]. In this work, AgNPs suspension at a concentration of 1000 µg/ml showed the highest anti-bacterial activity against tested MDR bacteria. The five MDR bacteria, *S. hemolytic* (U4), *K. pneumoniae* (U7), *S. hominis* (U11), *E. coli* (U8), and *K. pneumoniae* (U10) were observed to be the most sensitive to AgNPs, showing zones of inhibition of 24.33 ± 0.57, 23

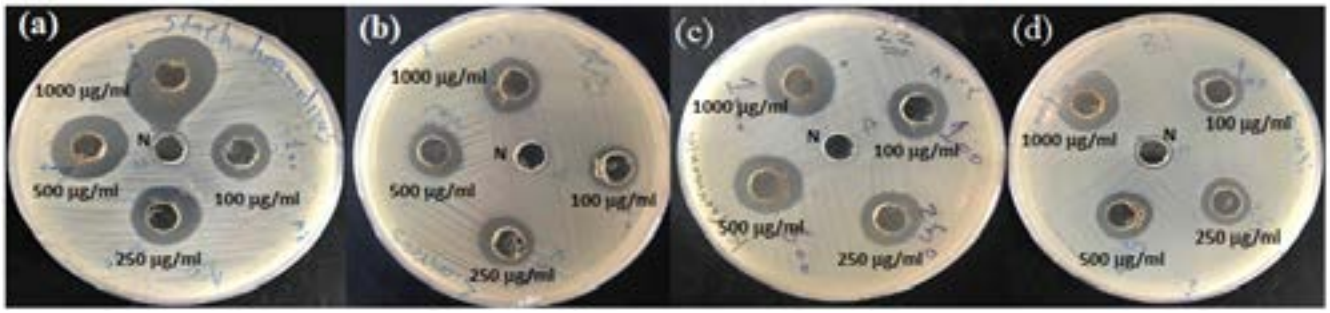

Figure 8: Anti-bacterial activity of AgNPs against some MDR bacteria. a: *S. haemolyticus* (U4) , b: *S.aureus* (U13), c: *K.pneumoniae* (U10), d: *E.coli* (U9), N: control (DMSO only)

Table 1: Anti-bacterial efficacy of *B.cereus* strain DBA1.1 AgNPs against MDR bacteria

Code of bacteria	*Name of bacteria*	*Concentrations of AgNPs (µg/mL) and zone of inhibition (mm)*			
		1000	*500*	*250*	*100*
U1	*E. faecalis*	16.33 ± 1.52^{a}	16.33 ± 0.57^{a}	14.67 ± 2.08^{a}	12.33 ± 0.57^{b}
U2	*E.coli*	17.33 ± 0.57^{a}	15 ± 1^{b}	14.33 ± 0.57^{bc}	12.67 ± 2.08^{c}
U3	*E. faecalis*	17 ± 1^{a}	15.67 ± 1.15^{a}	13 ± 2^{bc}	13.33 ± 0.57^{c}
U4	*S. haemolyticus*	24.33 ± 0.57^{a}	20.33 ± 1.52^{b}	18.67 ± 1.15^{b}	16 ± 1^{c}
U5	*K. pneumoniae*	18 ± 2^{a}	15.33 ± 0.57^{b}	14 ± 1^{b}	14.33 ± 0.57^{b}
U6	*E. coli*	18	± 0a 16 ± 0^{ac}	14.33 ± 2.51^{bc}	13 ± 1^{b}
U7	*K .pneumoniae*	23 ± 1^{a}	20.33 ± 0.57^{b}	17 ± 1^{c}	13.33 ± 1.52^{d}
U8	*E. coli*	21	± 1a 17 ± 1^{b}	15.33 ± 0.57^{bc}	14.33 ± 1.52^{c}
U9	*E. coli*	18.33 ± 1.52^{a}	15 ± 1^{b}	14.33 ± 1.52^{b}	13 ± 0^{b}
U10	*K. pneumoniae*	21.33 ± 0.57^{a}	18.33 ± 0.57^{b}	16	± 2c 15 ± 2^{c}
U11	*S. hominis*	22.33 ± 0.57^{a}	18 ± 1^{b}	15.33 ± 2.51^{c}	14.33 ± 1.52^{c}
U12	*K. oxytoca*	18			± 0a 16 ± 2ab 14 ± 0bc 13 ± 2^{c}
U13	*S. aureus*	16.33 ± 1.52^{a}	15.33 ± 0.57^{a}	14.33 ± 1.52^{a}	12 ± 2^{b}
U14	*S. hominis*	0			± 0a 0 ± 0a 0 ± 0a 0 ± 0^{a}
U15	*E. coli*	16.33 ± 0.57^{a}	15.33 ± 1.52^{a}	14.33 ± 0.57^{a}	12 ± 0^{b}
U16	*E. coli*	16 ± 0^{a}	15.33 ± 0.57^{ab}	13.33 ± 0.57^{bc}	12.33 ± 1.52^{c}

Note: For each tested MDR bacterium, values in the same row with different letters are significantly different (p.value ≤ 0.05), Mean ± SD, n=3

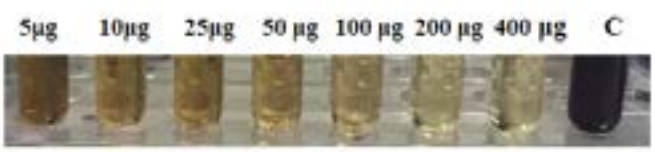

Figure 9: DPPH free radical scavenging of AgNPs at various concentrations (µg/mL). C: Control

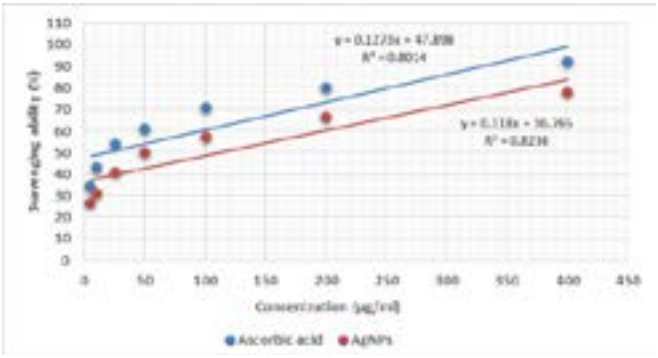

Figure 10: IC_{50} curve of AgNPs as compared with ascorbic acid

± 1, 22.33 ± 0.57, 21 ± 1 and 21.33 ± 0.57 mm, respectively. Mujaddidi *et al*. also found that MDR *Klebsiella pneumoniae* was the most sensitive to AgNPs, with inhibition zones of 18 mm at a concentration of 1000 µg/ ml [20].

In this study, fewer effects of AgNPs were observed against *E. feacalis* (U1), *S. aureus* (U13), *E. coli* (U15), and *E. coli* (U16), with inhibition zones of 16.33 ± 1.52 mm for both *E. feacalis* (U1) and *S. aureus* (U13), 16.33 ± 0.57 for *E. coli* (U15), and 16 ± 0 for *E. coli* (U16). The results of this study revealed that the anti-bacterial capacity of AgNPs against *S.aureus* (U13) and *E.coli* (U8) at all concentrations is higher than the activity of *Pseudomonas stutzerii* AgNPs synthesized in a recent study toward the same bacteria and at the same concentrations.[54] However, the anti-bacterial properties of AgNPs, depend on

Table 2: DPPH radical scavenging activity of AgNPs compared with ascorbic acid

Concentrations (µg/ml)	*Antioxidant activity of ascorbic acid (%)*	*Antioxidant activity of AgNPs (%)*
5	34.18 ± 1.18^{aa}	26.49 ± 1.99^{ba}
10	43.01 ± 1.03^{ab}	31.05 ± 3.00^{ba}
25	54.27 ± 1.07^{ac}	41.16 ± 1.84^{bb}
50	61.25 ± 1.15^{ad}	50.28 ± 3.92^{bc}
100	70.94 ± 3.04^{ae}	57.12 ± 4.08^{bd}
200	80.05 ± 1.10^{af}	66.38 ± 3.32^{be}
400	92.16 ± 0.96^{ag}	78.06 ± 2.02^{bf}
	IC_{50} = 16.51 µg/mL	IC_{50} = 112.16 µg/mL

Note: The values in the same row with different letters (black letters) and the values in the same column with different letters (red letters) are significantly different (p.value ≤ 0.05), Mean ± SD, n = 3

their charge [55], shape [56], and size [43].

In this work, *S. hominis* (U14) was resistant to all concentrations of AgNPs, and no inhibition zone was observed. This resistance may be attributed to multiple resistance mechanisms, such as permeability of the outer membrane, MDR efflux pumps, chromosomal resistance genes, as well as mutations and plasmid genes [57].

Antioxidant activity of the synthesized AgNPs

A DPPH radical scavenging assay was used to estimate the antioxidant activity of synthesized AgNPs at different concentrations (5, 10, 25, 50, 100, 200, 400 µg/mL). As shown in Figure 9, AgNPs managed to reduce purple DPPH to a yellow color, indicating potential free-radical scavenging abilities. DPPH comprises stable free radical molecules that can be easily reduced by receiving hydrogen or electrons from NPs.[58] In this study, the inhibition percentage of AgNPs increased as the concentration increased, where this result agrees with Riaz Rajoka *et al*.59 At the lowest concentration (5 µg/ml) of AgNPs, the percentage of scavenging activity was 26.49 ± 1.99%, increased to 78.06 ± 2.02% at the highest concentration (400 µg/mL), which is more effective than the antioxidant activity of AgNPs synthesized in previous work,[60] but less active compared to the other study[20] In the current study, the antioxidant activity of AgNPs was less effective than standard ascorbic acid (p.value ≤ 0.05) (Table 2). AgNPs had an IC_{50} value of 112.16 µg/mL, whereas ascorbic acid had an IC_{50} value of 16.51 µg/mL (Figure 10).

CONCLUSION

The extracellular synthesis of AgNPs was successfully accomplished using *B. cereus* strain DBA1.1 supernatant and the process was easy, inexpensive, and eco-friendly. Physical characterizations revealed that AgNPs were monodisperse, stable, spherical, and within acceptable sizes. Biosynthesized AgNPs demonstrated potent anti-bacterial activity against MDR bacteria isolated from UTI. Furthermore, the current study concluded that the AgNPs synthesized by *B. cereus* strain DBA1.1 were powerful free radical scavengers.

ACKNOWLEDGEMENT

The authors would like to thank the College of Nursing, University of Misan, for providing the laboratory instruments required to complete this study.

REFERENCE

1. Nadeem M, Khan R, Afridi K, Nachman A, Ullah S, Faisal S, et al. Green synthesis of cerium oxide nanoparticles (Ceo2 NPS) and their antimicrobial applications: A review. Int J Nanomedicine. 2020;15:5951–61.
2. Khan ZUH, Khan A, Chen Y, Shah NS, Muhammad N, Khan AU, et al. Biomedical applications of green synthesized Nobel metal nanoparticles. J Photochem Photobiol B Biol [Internet]. 2017;173:150–64.
3. Torres-Sangiao E, Holban AM, Gestal MC. Advanced nanomaterials: Vaccines, diagnosis, and treatment of infectious diseases. Molecules. 2016;21(7):1–22.
4. Slavin YN, Asnis J, Häfeli UO, Bach H. Metal nanoparticles: Understanding the mechanisms behind anti-bacterial activity. J Nanobiotechnology. 2017;15(1):1–20.
5. Khan I, Saeed K, Khan I. Nanoparticles: Properties, applications and toxicities. Arab J Chem [Internet]. 2019;12(7):908–31.
6. Jamkhande PG, Ghule NW, Bamer AH, Kalaskar MG. Metal nanoparticles synthesis: An overview on methods of preparation, advantages and disadvantages, and applications. J Drug Deliv Sci Technol [Internet]. 2019;53:101174.
7. Baig N, Kammakakam I, Falath W, Kammakakam I. Nanomaterials: A review of synthesis methods, properties, recent progress, and challenges. Mater Adv. 2021;2(6):1821–71.
8. Singh P, Kim YJ, Singh H, Mathiyalagan R, Wang C, Yang DC. Biosynthesis of anisotropic silver nanoparticles by Bhargavaea indica and their synergistic effect with antibiotics against pathogenic microorganisms. J Nanomater. 2015; 2015:1–15.
9. Singh P, Kim YJ, Wang C, Mathiyalagan R, Yang DC. Weissella oryzae DC6-facilitated green synthesis of silver nanoparticles and their antimicrobial potential. Artif Cells, Nanomedicine Biotechnol. 2016;44(6):1569–75.
10. Ovais M, Khalil AT, Islam NU, Ahmad I, Ayaz M, Saravanan M, et al. Role of plant phytochemicals and microbial enzymes in the biosynthesis of metallic nanoparticles. Appl Microbiol Biotechnol. 2018;102(16):6799–814.
11. Velusamy P, Kumar GV, Jeyanthi V, Das J, Pachaiappan R. Bio-inspired green nanoparticles: Synthesis, mechanism, and anti-bacterial application. Toxicol Res. 2016;32(2):95–102.
12. Klaus T, Joerger R, Olsson E, Granqvist CG. Silver-based crystalline nanoparticles, microbially fabricated. Proc Natl Acad Sci U S A. 1999;96(24):13611–4.
13. Van Tan L, Tran T, Thi VD. Biosynthesis of silver nanoparticles from Bacillus licheniformis TT01 isolated from quail manure collected in Vietnam. Processes. 2021;9(4):1–13.
14. Otari S V., Patil RM, Ghosh SJ, Thorat ND, Pawar SH. Intracellular synthesis of silver nanoparticle by actinobacteria and its antimicrobial activity. Spectrochim Acta - Part A Mol Biomol Spectrosc [Internet]. 2015;136:1175–80.
15. Abd-Elhalim B.T, Gamal R.F, Abou-Taleb kh.A, Haroun AA Biosynthesis of Copper nanoparticles using bacterial supernatant optimized with certain agro-industrial byproducts. Nov Res Microbiol J. 2019;3(6):558–78.
16. El-shanshoury AER, Ebeid E, Elsilk S, Ebeid ME. Biogenic Synthesis of Gold Nanoparticles by Bacteria and Utilization of the Chemical Fabricated for Diagnostic Performance of Viral Hepatitis C Virus-NS4. *Letters in Applied NanoBioScience*. 2020; 9, 1395-1408
17. Clifford K, Desai D, da Costa CP, Meyer H, Klohe K, Winkler A, et al. Antimicrobial resistance in livestock and poor quality veterinary medicines. Bull World Health Organ. 2018;96(9):662–4.
18. Poletajew S, Pawlik K, Bonder-Nowicka A, Pakuszewski A, Nyk Ł, Kryst P. Multi-drug resistant bacteria as aetiological factors of infections in a tertiary multidisciplinary hospital in Poland. Antibiotics. 2021;10(10):1–10.
19. Valentina Y. Optimisation of Reactant Concentration in Biosynthesis of Silver Nanoparticles using Pathogenic Bacteria Isolated from Clinical Sources and their Characterisation: A Recent Study. Innov Microbiol Biotechnol Vol 3. 2022;7(1):45–55.
20. Mujaddidi N, Nisa S, Al Ayoubi S, Bibi Y, Khan S, Sabir M, et al. Pharmacological properties of biogenically synthesized silver nanoparticles using endophyte Bacillus cereus extract of Berberis lyceum against oxidative stress and pathogenic multidrug-resistant bacteria. Saudi J Biol Sci [Internet]. 2021;28(11):6432–40.
21. Salem SS, Ali OM, Reyad AM, Abd-Elsalam KA, Hashem AH. Pseudomonas indica-Mediated Silver Nanoparticles: Antifungal and Antioxidant Biogenic Tool for Suppressing Mucormycosis Fungi. J Fungi. 2022;8(2):126
22. Ghali H Alshami A, Al-Tamimi WH, Hateet RR. Screening for extracellular synthesis of silver nanoparticles by bacteria isolated from Al-Halfaya oil field reservoirs in Missan province , Iraq. BIODIVERSITY. 2022; 23(7):3462–70.
23. Singh P, Kim YJ, Singh H, Wang C, Hwang KH, Farh MEA, et al. Biosynthesis, characterization, and antimicrobial applications of silver

nanoparticles. Int J Nanomedicine. 2015;10:2567–77.
24. Qais FA, Shafiq A, Khan HM, Husain FM, Khan RA, Alenazi B, et al. Anti-bacterial effect of silver nanoparticles synthesized using Murraya koenigii (L.) against multidrug-resistant pathogens. Bioinorg Chem Appl. 2019; 2019:1–11.
25. Saleh MN, Khoman Alwan S. Biosynthesis of silver nanoparticles from bacteria Klebsiella pneumonia: Their characterization and anti-bacterial studies. J Phys Conf Ser. 2020;1664(1):1–15.
26. Kotakadi VS, Gaddam SA, Venkata SK, Sarma PVGK, Sai Gopal DVR. Biofabrication and spectral characterization of silver nanoparticles and their cytotoxic studies on human CD34 +ve stem cells. 3 Biotech. 2016; 6(2):1–11.
27. Pallavi SS, Rudayni HA, Bepari A, Niazi SK, Nayaka S. Green synthesis of Silver nanoparticles using Streptomyces hirsutus strain SNPGA-8 and their characterization, antimicrobial activity, and anticancer activity against human lung carcinoma cell line A549. Saudi J Biol Sci [Internet]. 2022; 29(1):228–38.
28. Al-Naqshbandi AA, Chawsheen MA, Abdulqader HH. Prevalence and antimicrobial susceptibility of bacterial pathogens isolated from urine specimens received in rizgary hospital — Erbil. J Infect Public Health [Internet]. 2019;12(3):330–6.
29. Mollick S, Dasgupta T, Hasnain J, Ahmed M. Isolation and characterization of pathogens responsible for urinary tract infection in Bangladesh and determination of their antibiotic susceptibility pattern. J Appl Pharm Sci. 2016; 6(4):72–6.
30. CLSI. Performance Standards for Antimicrobial Susceptibility Testing. 31st ed. CLSI supplement M100. Informational Supplement M100-S31. [Internet]. Vol. 8, Journal of Services Marketing. 2021. 1–352 p.
31. Basak S, Singh P, Rajurkar M. Multidrug-Resistant and Extensively Drug-Resistant Bacteria: A Study. J Pathog. 2016; 2016:1–5.
32. Fouda A, EL-Din Hassan S, Salem SS, Shaheen TI. In-Vitro cytotoxicity, anti-bacterial, and UV protection properties of the biosynthesized Zinc oxide nanoparticles for medical textile applications. Microb Pathog [Internet]. 2018;125:252–61.
33. Elbeshehy EKF, Elazzazy AM, Aggelis G. Silver nanoparticles synthesis mediated by new isolates of Bacillus spp ., nanoparticle characterization and their activity against Bean Yellow Mosaic Virus and human pathogens. Front Microbiol. 2015;6:1–13.
34. Syed B, Nagendra Prasad MN, Satish S. Synthesis and characterization of silver nanobactericides produced by Aneurinibacillus migulanus 141, a novel endophyte inhabiting Mimosa pudica L. Arab J Chem [Internet]. 2019;12(8):3743–52.
35. Gloria Martin KD, Vergara Padilla KG. Sunlight Mediated Synthesis of Silver Nanoparticles by Bacillus sp and Its Anti-bacterial Property. Orient J Chem. 2020;36(03):419–24.
36. Shanshoury AERE, Sabae SZ, Shouny WAE, Shady AMA, Badr HM. Extracellular biosynthesis of silver nanoparticles using aquatic bacterial isolate and its anti-bacterial and antioxidant potentials. Egypt J Aquat Biol Fish. 2020;24(7 Special issue):183–201.
37. Koul B, Poonia AK, Yadav D, Jin JO. Microbe-mediated biosynthesis of nanoparticles: Applications and future prospects. Biomolecules. 2021;11(6):1–33.
38. Singh H, Du J, Singh P, Yi TH. Extracellular synthesis of silver nanoparticles by Pseudomonas sp. THG-LS1.4 and their antimicrobial application. J Pharm Anal [Internet]. 2018;8(4):258–64.
39. Sathiya CK, Akilandeswari S. Fabrication and characterization of silver nanoparticles using Delonix elata leaf broth. Spectrochim Acta - Part A Mol Biomol Spectrosc [Internet]. 2014;128:337–41. Available from: http://dx.doi.org/10.1016/j.saa.2014.02.172
40. Alsamhary KI. Eco-friendly synthesis of silver nanoparticles by Bacillus subtilis and their anti-bacterial activity. Saudi J Biol Sci [Internet]. 2020;27(8):2185–91.
41. Jahan I, Erci F, Isildak I. Rapid green synthesis of non-cytotoxic silver nanoparticles using aqueous extracts of "Golden Delicious" apple pulp and cumin seeds with anti-bacterial and antioxidant activity. SN Appl Sci [Internet]. 2021;3(1):1–14. Available from: https://doi.org/10.1007/s42452-020-04046-6
42. Alahmad A, Feldhoff A, Bigall NC, Rusch P, Scheper T, Walter JG. Hypericum perforatum L.-mediated green synthesis of silver nanoparticles exhibiting antioxidant and anticancer activities. Nanomaterials. 2021;11(2):1–26.
43. Hanna AL, Hamouda HM, Goda HA, Sadik MW, Moghanm FS, Ghoneim AM, et al. Biosynthesis and Characterization of Silver Nanoparticles Produced by Phormidium ambiguum and Desertifilum tharense Cyanobacteria. Bioinorg Chem Appl. 2022;2022:1–18.
44. Mondal AH, Yadav D, Mitra S, Mukhopadhyay K. Biosynthesis of silver nanoparticles using culture supernatant of Shewanella sp. ARY1 and their anti-bacterial activity. Int J Nanomedicine. 2020;15:8295–310.
45. Huq MA, Akter S. Biosynthesis, characterization and anti-bacterial application of novel silver nanoparticles against drug-resistant pathogenic klebsiella pneumoniae and salmonella enteritidis. Molecules. 2021;26(19):1–17.
46. Ahmed T, Shahid M, Noman M, Niazi MBK, Mahmood F, Manzoor I, et al. Silver nanoparticles synthesized by using Bacillus cereus SZT1 ameliorated the damage of bacterial leaf blight pathogen in rice. Pathogens. 2020;9(3):1–17.
47. Marooufpour N, Alizadeh M, Hatami M, Asgari Lajayer B. Biological Synthesis of Nanoparticles by Different Groups of Bacteria. Nanotechnol Life Sci. 2019; 63–85.
48. Fouad H, Hongjie L, Yanmei D, Baoting Y, El-Shakh A, Abbas G, et al. Synthesis and characterization of silver nanoparticles using Bacillus amyloliquefaciens and Bacillus subtilis to control filarial vector Culex pipiens pallens and its antimicrobial activity. Artif Cells, Nanomedicine Biotechnol [Internet]. 2017;45(7):1369–78.
49. Saravanan M, Barik SK, Mubarak Ali D, Prakash P, Pugazhendhi A. Synthesis of silver nanoparticles from Bacillus brevis (NCIM 2533) and their anti-bacterial activity against pathogenic bacteria. Microb Pathog [Internet]. 2018;116:221–6.
50. Ibrahim E, Fouad H, Zhang M, Zhang Y, Qiu W, Yan C, et al. Biosynthesis of silver nanoparticles using endophytic bacteria and their role in inhibition of rice pathogenic bacteria and plant growth promotion. RSC Adv. 2019; 9(50): 29293–9.
51. Patil S, Chandrasekaran R. Biogenic nanoparticles: a comprehensive perspective in synthesis, characterization, application and its challenges. J Genet Eng Biotechnol. 2020;18(1):1–23.
52. Qing Y, Cheng L, Li R, Liu G, Zhang Y, Tang X, et al. Potential anti-bacterial mechanism of silver nanoparticles and the optimization of orthopedic implants by advanced modification technologies. Int J Nanomedicine. 2018;13:3311–27.
53. Yin IX, Zhang J, Zhao IS, Mei ML, Li Q, Chu CH. The anti-bacterial mechanism of silver nanoparticles and its application in dentistry. Int J Nanomedicine. 2020;15:2555–62.
54. Bachii SA, Sahib WHA, Abd A, Razaq AL. Preparation and Characterization of Silver Nanoparticles Biosynthesis by Pseudomonas stutzeri Environmental Bacteria Isolated from Oil Fields and Their Antimicrobial Activity. Sci J Med Res. 2021;5(17):7–15.
55. Abbaszadegan A, Ghahramani Y, Gholami A, Hemmateenejad B, Dorostkar S, Nabavizadeh M, et al. The effect of charge at the surface of silver nanoparticles on antimicrobial activity against gram-positive and gram-negative bacteria: A preliminary study. J Nanomater. 2015; 2015:1–8.
56. Tang S, Zheng J. Anti-bacterial Activity of Silver Nanoparticles : Structural Effects. Adv Healthc Mater. 2018; 7(13), 1701503.
57. Salas-Orozco M, Niño-Martínez N, Martínez-Castañón GA, Méndez FT, Jasso MEC, Ruiz F. Mechanisms of resistance to silver nanoparticles in endodontic bacteria: A literature review. J Nanomater. 2019;2019:1–11.
58. Patil MP, Kang M jae, Niyonizigiye I, Singh A, Kim JO, Seo YB, et al. Extracellular synthesis of gold nanoparticles using the marine bacterium Paracoccus haeundaensis BC74171T and evaluation of their antioxidant activity and antiproliferative effect on normal and cancer cell lines. Colloids Surfaces B Biointerfaces [Internet]. 2019;183:110455.
59. Riaz Rajoka MS, Mehwish HM, Zhang H, Ashraf M, Fang H, Zeng X, et al. Anti-bacterial and antioxidant activity of exopolysaccharide mediated silver nanoparticle synthesized by Lactobacillus brevis isolated from Chinese koumiss. Colloids Surfaces B Biointerfaces [Internet]. 2020;186:110734.
60. Abhang P. Antimicrobial and Antioxidant Properties of Silver Nanoparticles Synthesized from Escherichia coli. Sci Technol Dev. 2020; 9(7); 54–61.